Short range stationary patterns and long range disorder in an evolution equation for one-dimensional interfaces

Javier Muñoz-García,[1] Rodolfo Cuerno,[1] and Mario Castro[2]

[1] *Departamento de Matemáticas and Grupo Interdisciplinar de Sistemas Complejos (GISC), Universidad Carlos III de Madrid, Avenida de la Universidad 30, E-28911 Leganés, Spain*
[2] *GISC and Grupo de Dinámica No Lineal (DNL), Escuela Téc. Sup. de Ingeniería (ICAI), Universidad Pontificia Comillas, E-28015 Madrid, Spain*

(Dated: February 6, 2008)

A novel local evolution equation for one-dimensional interfaces is derived in the context of erosion by ion beam sputtering. We present numerical simulations of this equation which show interrupted coarsening in which an ordered cell pattern develops with constant wavelength and amplitude at intermediate distances, while the profile is disordered and rough at larger distances. Moreover, for a wide range of parameters the lateral extent of ordered domains ranges up to tens of cells. This behavior is new in the context of dynamics of surfaces or interfaces with morphological instabilities. We also provide analytical estimates for the stationary pattern wavelength and mean growth velocity.

PACS numbers: 47.54.-r, 68.35.Ct, 05.45.-a, 79.20.Rf, surfaces

Pattern formation is ubiquitous in nature and one of the most fascinating features of nonequilibrium systems [1]. Typical examples can be found in many startlingly similar interfaces which emerge in very different processes, such as growth of amorphous [2] and epitaxial thin films [3], or erosion by ion beam sputtering (IBS) [4]. These pattern forming surfaces can be classified into different categories according to the stationary or time-dependent (coarsening) behavior of the typical pattern length scale l. Actually, a large effort has been devoted recently to describe these systems through height equations [5], since these provide compact and efficient analytical/numerical descriptions that successfully describe global morphological properties such as kinetic roughening, and surface pattern formation and coarsening. Specifically, in order to assess the predictive power of ($1d$) height equations, it would be important to produce criteria for the presence or absence of coarsening. In Ref. [6] up to four different scenarios have been proposed depending on the behavior of l as a function of the pattern amplitude A. The conclusion is that coarsening stops (*interrupted coarsening*) if the function $l(A)$ attains a maximum, after which the amplitude increases indefinitely with time. A similar conclusion was reached at by Krug in Ref. [7], where it is actually conjectured that no ($1d$) *local* height equation can "describe the emergence and evolution of patterns with constant wavelength *and* amplitude". Hence, a $1d$ counterexample of an interface equation [5] leading to a stationary pattern with constant wavelength and amplitude would be interesting to improve our understanding of interrupted coarsening and, specifically, of the type of nonlinearities that induce it [8].

Recently, a continuum 2d model has been introduced which describes interesting (sub)micrometric features of surfaces eroded by IBS [9, 10]. The resulting interface equation was studied numerically for moderate system sizes suggesting the occurrence of a stationary ordered pattern and interrupted coarsening [11]. Here, we derive the $1d$ counterpart of the height equation in [10] from a physical model of IBS and perform a systematic numerical analysis of its coarsening properties in relation with Krug's conjecture.

Following the standard assumption made in hydrodynamic models of aeolian sand dunes [12], we will consider that ripples formed under IBS are translationally invariant in the y direction; additionally, we assume symmetry under $x \to -x$, as occurs under normal incidence conditions for the bombarding ions [13]. As proposed in [10], the evolution of the thickness of the mobile surface adatoms layer R and the height of the bombarded surface h is provided by a pair of coupled equations, namely,

$$\partial_t R = (1-\phi)\Gamma_{ex} - \Gamma_{ad} + D\partial_x^2 R, \qquad (1)$$

$$\partial_t h = -\Gamma_{ex} + \Gamma_{ad}, \qquad (2)$$

where Γ_{ex} and Γ_{ad} are, respectively, rates of atom excavation from and addition to the immobile bulk, $(1-\phi)$ measures the fraction of eroded atoms that become mobile, and the third term in Eq. (1) describes thermal diffusion of mobile adatoms.

The rate at which material is sputtered from the bulk is described by microscopic derivations [14] and depends on the local morphology of the surface

$$\Gamma_{ex} = \alpha_0\left[1 + \alpha_2\partial_x^2 h + \alpha_3(\partial_x h)^2\right], \qquad (3)$$

where α_0 is the sputtering rate for a planar surface. The rate of nucleation is also related to the local shape of the surface, and is given by

$$\Gamma_{ad} = \gamma_0\left[R(1+\gamma_2\partial_x^2 h) - R_{eq}\right], \qquad (4)$$

where R_{eq} is the thickness due to the mobile atoms that are thermally generated even in the absence of

bombardment, and γ_0^{-1} is the average time between nucleation events. After a multiple scale expansion of (1)-(4), R can be adiabatically eliminated from Eqs. (1) and (2) [9, 10], obtaining, to lowest order near threshold of the morphological instability, the following $1d$ equation for the evolution of the surface height,

$$\partial_t h(x,t) = -\nu\partial_x^2 h - K\partial_x^4 h + \lambda_1(\partial_x h)^2 - \lambda_2\,\partial_x^2(\partial_x h)^2, \quad (5)$$

where parameters are related to those in (1)-(4) and depend on the experimental conditions. To the best of our knowledge, the *deterministic* Eq. (5) has not been systematically studied. We will restrict ourselves to positive values of ν and K, which are required in order to produce a long-wavelength instability. Moreover, λ_1 and λ_2 are required to have the same sign for mathematical well-posedness, as shown in [15, 16]. If the signs of the non-linear terms are simultaneously changed, Eq. (5) remains invariant after $h \to -h$. Thus, we will only consider positive values of these parameters. For $\lambda_2 = 0$, Eq. (5) reduces to the celebrated Kuramoto-Sivashinsky (KS) equation [17, 18], which is a paradigm of spatio-temporal chaos. Its nonlinear term stabilizes the system and a (disordered) pattern develops that is characterized by a wavelength that does *not* coarsen, and by chaotic cell dynamics. On large length scales, the KS system can be effectively described by the *stochastic* Kardar-Parisi-Zhang (KPZ) equation [19], paradigmatic of kinetic roughening. In particular, the surface roughness (global rms width, W) [20] for a KPZ interface scales as a power law with the lateral system size L. On the other hand, for $\lambda_2 \neq 0$ and $\lambda_1 = 0$, Eq. (5) reduces to the "conserved" KS equation. This equation has been studied in the context of amorphous thin film growth [15] and step dynamics on vicinal surfaces [21]; in this case, the linear instability evolves into an *ordered* pattern of paraboloids with *uninterrupted* coarsening.

In order to reduce the number of parameters and simplify the analysis of (5), we rescale x, t and h by $(K/\nu)^{1/2}, K/\nu^2$ and ν/λ_1, respectively, resulting into a single-parameter equation, namely,

$$\partial_t h(t,x) = -\,\partial_x^2 h - \partial_x^4 h + (\partial_x h)^2 - r\,\partial_x^2(\partial_x h)^2, \quad (6)$$

where $r = (\nu\lambda_2)/(K\lambda_1)$ is the (squared) ratio of a linear crossover lengthscale to a non-linear crossover lengthscale. We have performed a numerical integration of (6) using a fourth-order Runge-Kutta method and the improved spatial discretization introduced by Lam and Shin [22] for the nonlinear terms. We have used periodic boundary conditions, lattice constant $\Delta x = 0.5$ and time step $\Delta t = 0.01$, checking that results do not differ significantly for smaller space and time steps. The initial height values were chosen uniformly distributed between 0 and 1 and statistical data were obtained as averages over 250 random initial conditions. The standard system size of our simulations was $L = 512$ (1024 nodes), except when other values are indicated, and the parameters fixed to $\nu = 1$, $K = 1$, $\lambda_1 = 0.1$, varying λ_2 in order to check for the different values of r.

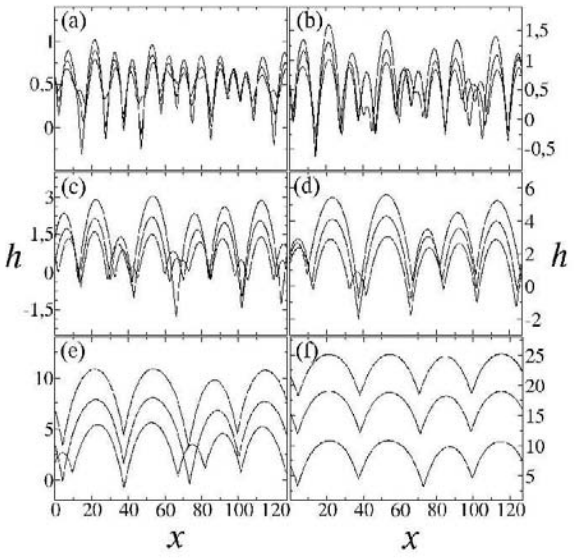

FIG. 1: Height profiles for Eq. (6) with $r = 50$ on a system size $L = 128$ at times (a) $t = 2$, 6, 11; (b) $t = 11$, 24, 41; (c) $t = 41$, 70, 103; (d) $t = 103$, 153, 205; (e) $t = 205$, 302, 425; (f) $t = 425$, 764, 1024. Height profiles at different times evolve by increasing the maximum value of h with time. All units are arbitrary.

In Fig. 1 the evolution of the height profile is depicted for $r = 50$. Starting from an initial random distribution, a periodic surface structure with a wavelength of about the maximum of the linear dispersion relation [1], namely $l_{linear} = 2\sqrt{2}\pi$, arises and the amplitude of h increases (Fig. 1a). At later stages, the *conserved* KPZ nonlinearity $\partial_x^2(\partial_x h)^2$ (cKPZ) induces coarsening of the ordered cell-like structure, wherein the cells grow in width and height and the number of cells decreases. This coarsening is such that smaller cells are "eaten" by larger neighbors (Figs. 1b-e). We show in Fig. 2a the time evolution of the mean height $\bar{h}_L(t) = 1/L\sum_x h(x,t)$, the wavelength $l(t)$, and the amplitude $A(t)$ of the pattern defined as the mean lateral distance between two consecutive local minima and the mean vertical distance from a local minimum to the next local maximum, respectively. As seen in Fig. 2a, for $t \gtrsim 70$, the *non-conserved* KPZ term $(\partial_x h)^2$ becomes relevant and the mean height of the surface $\bar{h}_L$ starts increasing to reach a constant velocity (Fig. 1f). At the same time, the coarsening process slows down until stopping completely in the stationary state. This behavior suggests that the cKPZ term, which

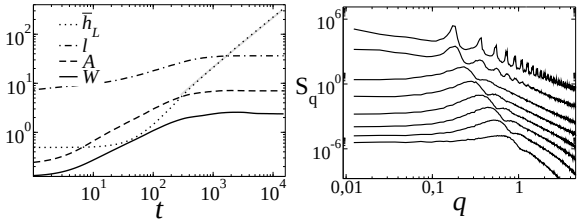

(a) (b)

FIG. 2: (a) Time evolution of mean surface height average $\bar{h}_L(t)$, wavelength $l(t)$, amplitude $A(t)$, and global width $W(t)$, for $r = 50$; (b) corresponding surface structure factor as a function of wave number q at times $t = 4, 15, 30, 60, 125, 250, 1129$, and 10653, bottom to top (curves are offset vertically). All units are arbitrary.

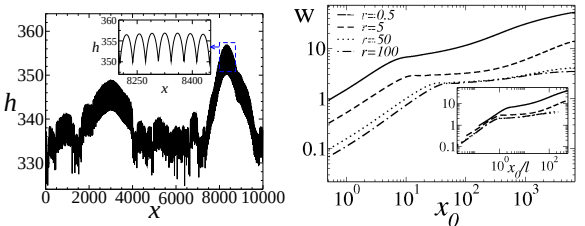

(a) (b)

FIG. 3: (a) Height profile at $t = 15000$ for a system size $L = 10000$ and $r = 50$; (b) local width vs window size at $t = 15000$ for several values of r and $L = 8192$. Inset: same data plotted vs $x_0/(2\sqrt{6r})$. All units are arbitrary.

acts at small scales, induces the order and the coarsening process until the slopes and the characteristic wavelength of the pattern are large enough to make the KPZ term no longer negligible. At this time, the KPZ term interrupts the coarsening process, as claimed in [8, 10], and a constant average velocity value is achieved as a consequence of a constant average of slopes across the interface. Thus, the final wavelength of the pattern depends on the interplay between the cKPZ and the KPZ terms. Fig. 2a also shows the global surface rms width or roughness $W(t)$ [20], and Fig. 2b shows the surface structure factor, defined as $S(q,t) = \left\langle \hat{h}(q,t)\hat{h}(-q,t) \right\rangle$, where $\hat{h}(q,t)$ is the Fourier transform of the field $h(x,t)$.

The first peak in the structure factor indicates the dominant wavelength of the pattern. We can see how this peak moves to larger wavelengths (coarsening) until a fixed mode is reached which corresponds to the stationary value $l \approx 36$ in Fig. 2a. At this time coarsening interrupts and the amplitude saturates to a constant value. Nevertheless, for large enough L and at long distances, the profile disorders in heights (Fig. 3a), although the lateral cell-like order is still preserved for intermediate distances (Fig. 3a, inset; note the difference in scales between the x and y axes). This disorder reflects in the power law behavior of $S(q,t)$ for q much smaller than $2\pi/l$ and long enough times (Fig. 2b) or, equivalently, in the behavior of the local width $w(x_0)$ [20] at long times, displayed in Fig. 3b as a function of window size, x_0. Due to the parabolic shape of the cells, the local width scales as $w \sim x_0^2$ for distances smaller than the cell size, reaching a plateau for intermediate distances, and finally increasing as a (smaller) power of x_0 for large enough distances (kinetic roughening). The plateau in $w(x_0)$ is related to the lateral order of the pattern, reaching up to several tens of cells (see e.g. in Fig. 4a an ordered domain containing over 30 cells for $r = 10$). The effective exponent characterizing the long distance behavior of $w(x_0)$ increases towards its KS value (1/2) for decreasing r. Indeed, the profile is more disordered for small r, as can be observed from Fig. 4a, to the extent that for $r \approx 0.2$, and independently of L, the secondary peaks in the structure factor vanish completely (not shown), and only a weak peak about the linear instability persists, as in the KS equation. Thus, the KPZ term is seen to act at larger scales and is responsible for the disorder of the profile, while the cKPZ terms dominates at smaller scales with a trend to order the cells vertically.

As indicated above, for large r values and after the initial times, the cell-like structure is well ordered and the length scales of the profile are large enough so that the linear fourth order derivative can be effectively neglected. Thus, we can rescale $x \to r^{1/2}x$, $t \to rt$ and $h \to h$ to obtain an effective parameter-free equation. This means that, for large values of r, the solution of Eq. (6) remains unchanged if we rescale lengths by $r^{1/2}$ and times by r. In order to check this hypothesis we present in Fig. 4b the final amplitude and wavelength of the structure for different values of r. We can observe that, for large values of r, the height amplitude does not change with r and the wavelength l is proportional to $r^{1/2}$ as predicted above. This behavior can be also seen in the inset of Fig. 3b, where we rescale the horizontal axis by $l = 2\sqrt{6r}$ (see below), obtaining almost perfect collapse of the curves for large r.

Further progress can be made by recalling that the solution of (5) with $\lambda_1 = 0$ is a periodic juxtaposition of parabolas of the form [15, 21]

$$h(x) = A - \frac{4A}{l^2}\, x^2. \tag{7}$$

We can consider this function as an approximate solution of Eq. (6) for large values of r. In Fig. 5a we compare the numerical profile with the function (7) for $r = 50$. Using this solution and assuming as a condition for the final (interrupted) structure that the averaged nonlinear contributions along one period must be equal, we obtain a relation between

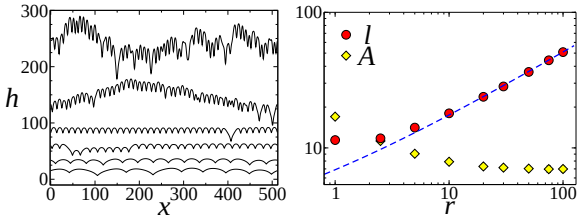

(a) (b)

FIG. 4: (a) Height profiles at $t = 15000$ for (top to bottom) $r = 0.1, 0.5, 1, 5, 10, 50$, and 100; (b) stationary wavelength l and amplitude A as functions of r (statistical errors are smaller than the symbol sizes). The dashed line corresponds to $l = 2\sqrt{6r}$. All units are arbitrary.

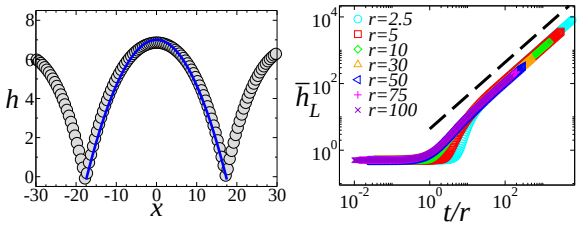

(a) (b)

FIG. 5: (a) Stationary height profile at $t = 15000$ for $r = 50$. The solid line represents the approximate solution given by (7) for $l = 2\sqrt{6r}$ and $A = 7$; (b) mean height for different values of r as a function of t/r. The dashed line is given by (8). All units are arbitrary.

the final wavelength and r, namely $l = 2\sqrt{6r}$. This function is represented in Fig. 4b, fitting accurately the stationary wavelengths obtained numerically for large values of r. The net mean growth velocity of the height average is only due to the KPZ nonlinear term and is given by $v = \left\langle \lambda_1 \overline{[\partial_x h(x)]^2}_L \right\rangle$. Assuming (7) as an approximate solution and integrating over one period, we obtain the net mean profile evolution. It reads

$$\bar{h}_L(t) = vt \approx \lambda_1 \left\{ \frac{1}{l} \int_{-l/2}^{l/2} \left[\partial_x h(x)\right]^2 dx \right\} t = \lambda_1 \frac{11}{r} t, \tag{8}$$

where we have substituted $l = 2\sqrt{6r}$, and $A \approx 7$ is obtained from Fig. 4b. As seen from Fig. 5b, for large values of r the evolution of $\bar{h}_L$ becomes r-independent if we rescale $t \to rt$, as already indicated. Furthermore, at long times, the growth velocity given by (8) agrees accurately with the numerical observations for a wide range in r.

In conclusion, we have derived a novel deterministic $1d$ equation with shift symmetry in the context of ion-beam sputtering and performed a numerical analysis to obtain some relevant information about its solutions. For large values of r we have estimated the final pattern wavelength assuming a parabolic solution analogous to that of the "conserved" KS equation and checked our assumption by comparing with the numerical mean height evolution. The resulting single-parameter Eq. (6) interpolates between the KS equation for $r = 0$, which presents a chaotic solution and no coarsening, and the "conserved" KS equation for $r \to \infty$ (upon rescaling $h \to h/r$), which displays unbounded coarsening. This behavior is similar to the $1d$ *convective* Cahn-Hilliard (cCH) equation studied in [23]. However, as reported in Ref. [23], coarsening does not interrupt in the cCH system for a whole range of parameter values but, rather, proceeds logarithmically for long times, whereas Eq. (6) does present interrupted coarsening with an *ordered pattern* of constant wavelength and amplitude *for intermediate distances*. This behavior provides a new scenario for the classification of surface coarsening phenomena in Ref. [6], where all the studied evolution equations display perpetual coarsening, or else develop a pattern with a frozen wavelength while the amplitude continues growing without bound in the course of time. Regarding Krug's conjecture [7], the present example reinforces its validity for long range order properties, since the pattern produced by Eq. (6) disorders at large length scales. However, our results suggest that it is still possible to stabilize a well ordered pattern over (intermediate) distances ranging even up to several tens of cell sizes in contrast with other equations in this context.

Acknowledgments

This work has been partially supported by MEC (Spain), through Grants Nos. BFM2003-07749-C05, -01, -05, and the FPU programme (J.M.-G.).

[1] M. C. Cross and P. C. Hohenberg, Rev. Mod. Phys. **65**, 851 (1993).
[2] A.-L. Barabási and H. E. Stanley, *Fractal Concepts in Surface Growth* (Cambridge University Press, 1995).
[3] P. Politi *et al.*, Phys. Rep. **324**, 271 (2000).
[4] U. Valbusa, C. Boragno, and F. B. de Mongeot, J. Phys.: Condens. Matter **14**, 8153 (2002).
[5] We take "interface" or "height" equation in the restricted sense that physics is invariant under global height shifts $h(x,t) \to h(x,t) + const.$
[6] P. Politi and C. Misbah, Phys. Rev. Lett. **92**, 090601

(2004); Phys. Rev. E **73**, 036133 (2006).
[7] J. Krug, Adv. Compl. Sys. **4**, 353 (2001).
[8] M. Castro *et al.*, submitted (2006).
[9] M. Castro *et al.*, Phys. Rev. Lett. **94**, 016102 (2005).
[10] J. Muñoz-García, M. Castro, and R. Cuerno, Phys. Rev. Lett. **96**, 086101 (2006).
[11] The *stochastic* version of this 2d equation was previously derived in the context of amorphous thin film growth, see M. Raible *et al.*, Europhys. Lett. **50**, 61 (2000); M. Raible, S. Linz, and P. Hänggi, Phys. Rev. E **64**, 031506 (2001).
[12] O. Terzidis, P. Claudin and J.-P. Bouchaud, Eur. Phys. J. B **5**, 245 (1998); A. Valance and F. Rioual, Eur. Phys. J. B **10**, 543 (1999); Z. Csahók *et al.*, Eur. Phys. J. E **3**, 71 (2000).
[13] S. Facsko *et al.*, Science **285**, 1551 (1999); R. Gago *et al.*, Appl. Phys. Lett. **78**, 3316 (2001).
[14] R. M. Bradley and J. M. Harper, J. Vac. Sci. Technol. A **6**, 2390 (1988); R. Cuerno and A.-L. Barabási, Phys. Rev. Lett. **74**, 4746 (1995); M. Makeev, R. Cuerno, and A.-L. Barábasi, Nucl. Instrum. Methods Phys. Res., Sect. B **197**, 185 (2002).
[15] M. Raible, S. J. Linz, and P. Hänggi, Phys. Rev. E **62**, 1691 (2000).
[16] M. Castro and R. Cuerno, Phys. Rev. Lett. **94**, 139601 (2005).
[17] G. I. Sivashinsky, Ann. Rev. Fluid Mech. **15**, 179 (1983).
[18] Y. Kuramoto, *Chemical Osillation, Waves and Turbulence* (Springer, Berlin, 1984).
[19] K. Sneppen *et al.*, Phys. Rev. A **46**, R7351 (1992).
[20] By defining *l*ocal width as $w^2(x_0) = \left\langle \sum_x \left[h(x,t) - \bar{h}_{x_0}\right]^2 / x_0 \right\rangle$ we have $W = w(x_0 = L)$.
[21] T. Frisch and A. Verga, Phys. Rev. Lett. **96**, 166104 (2006).
[22] C.-H. Lam and F. G. Shin, Phys. Rev. E **58**, 5592 (1998).
[23] A. A. Golovin *et al.*, Phys. Rev. Lett. **86**, 1550 (2001).

This figure "fig1.gif" is available in "gif" format from:

http://arXiv.org/ps/cond-mat/0701568v1